Scalable Production of Stabilized Catalysts via Atomic Layer Deposition

A. Goulas[*], A. Dokania[**], F. Grillo[**], J.R. van Ommen[**] and B. van Limpt[*]

[*]Delft IMP, Julianalaan 136, 2628 BL, Delft The Netherlands
[**]Delft University of Technology, ChemE, Product and Process Engineering, Julianalaan 136, 2628 BL, Delft, The Netherlands, j.r.vanommen@tudelft.nl

ABSTRACT

We report the fabrication of ultrathin aluminum-based overcoats on supported platinum catalysts using atomic layer deposition and hydrid atomic/molecular layer deposition. Tuning the process parameters and applying heat treatment for porosity induction can result to controllably accesible model catalysts. We examined the effect of the number of deposition cycles (1-25), co-reactant choice (water, ethylene glycol, 1,5-pentanediol) and exposure time on the characteristics of the alumina and alucone stabilizing films. The use of fluidized bed reactors for atomic layer deposition applied for active phase deposition and overcoat stabilization paves the way for large-scale gas-phase production of tailored nanostructured catalysts.

Keywords: Atomic Layer Deposition (ALD), heterogeneous catalysis, catalyst stability, platinum (Pt) nanoparticles, alumina (Al_2O_3) overcoat

1 INTRODUCTION

Optimizing catalyst performance at the atomic level can have a tremendous impact on the intensification of chemical processes. Tuning composition and structure parameters of the active species (size/dispersion, shape, position) during synthesis is one of the main objectives of catalyst nanostructuring [1]. As a result, more active, selective and stable catalysts with limited deactivation problems at demanding conditions (temperature, pressure, pH) can be obtained [2]. Additional advantages are minimizing the use of scarce and expensive materials (e.g. noble metals) and reducing the amount of waste related with the catalyst production process. In the past years, atomic layer deposition (ALD) has emerged as a nanostructuring toolbox for the modification of surface properties with atomic precision [3-5]. Already, support modification [6-8], nanoparticle decoration [5-13] and ultrathin-film overcoats *via* ALD have been used to effectively synthesize and stabilize noble [5-9, 13-17] and base metal [18-23] supported catalysts. Molecular layer deposition (MLD), the organic counterpart of ALD, has also been used in hybrid schemes for creating porous catalyst overcoats.[10-12] With these schemes, several enhanced catalysts with metal oxide and hybrid organic/inorganic overcoats have already been reported as shown in table 1.

Feng *et al.* [6] reported the application of 1 or 2 ALD cycles of TMA/H_2O to improve the behavior of Pd-ZnO/Al_2O_3 catalysts in methanol decomposition. The authors initially claimed that TMA would not react with the Pd clusters, thus resulting in selective coating of the ZnO support. The influence of the number of ALD cycles on the activity of the catalyst and the mobility of the metal clusters was further studied [7-8] and the low GPC observed (0.8 Å/cycle) was correlated to non-uniformity of the surface coverage. Liang *et al.* [11] applied alucone MLD overcoats to stabilize Pt clusters up to 800 ºC. The overcoats were rendered porous after calcination in air. Moreover, evidence for preferential coverage of the most energetic metal sites (edges, corners) during overcoat growth was indicated. Lu *et al.* [15] demonstrated the applicability of ALD overcoats on conventional catalysts. An accesible film of Al_2O_3 greatly improved the performance of Pd/Al_2O_3 catalysts in ethane oxidative dehydrogenation (ODH) by minimizing coking and sintering of the active phase.

The importance of overcoats for stabilization of catalysts used in liquid-phase reactions was recently discussed [20] further highlighting the importance of the calcination treatment for porosity induction *via* crystallization of the ALD overcoat. Additionally, the porous overoat films enhanced the performance of the catalyst to size-selective reactions due to the ability to tune the pore size [12]. The possiblity of adding acidity modifier such as MgO_x was also demonstrated. More bifunctional catalysts based on the growth of binary oxides have also been reported [18]. Finally, the use of blocking agents for selective growth of protective nanocages and selective nanobowls was introduced [5, 9]. A comprehensive review article [24] on the possibilies of ALD for catalyst design was recently communicated by O'Neill *et al.*

overcoat	reaction	reference
AlO_x	CH_3OH decomposition	[6-8]
alucone	CO oxidation	[11]
AlO_x	C_2H_6 ODH	[14-15]
AlO_x, MgO_x, NbO_x, TiO_x, alucone	furfural, C_4H_6, C_6H_{12} and $(CH_2)_8$ hydrogenation	[12-13, 17-20, 22-23]
alucone	CH_4 dry reforming	[10]
ZrO_x	O_2 reduction	[9]

Table 1: Reported ALD catalyst overcoats for enhancement of catalytic chemical reactions.

2 EXPERIMENTAL SECTION

The model catalysts were synthesized on titania nanoparticles (Aeroxide TiO_2 P 25, Evonik Industries, ~10 g) which are non-porous (specific surface area of 52 m^2/g) and have an average primary particle size of 21 nm. Prior using them in the ALD reactor for the Pt deposition, the nanoparticles were dried at 150 ºC for 4 hours in a muffle furnace and sieved (45 μm). For the growth of the active metal phase (Pt) and the protective Al-based overcoats a custom-built fluidized bed reactor operating in atmospheric pressure described elsewhere [25] was used. ALD of Pt was performed using alternative exposures to (trimethyl) methylcyclopentadienyl-platinum(IV) ($MeCpPtMe_3$, Strem Chemicals) and pre-heated dry synthetic air (Linde Gas Benelux) at a deposition temperature of 250 ºC. The Pt precursor was contained in a stainless steel bubbler and vaporization was carried at 70 ºC.For the overcoating experiments, ~1 g of particles were *in-situ* dried in the ALD reactor at 120 ºC in order to remove possibly physisorbed water. ALD of Al_2O_3 was performed using alternative exposures to trimethyl aluminium (TMA semiconductor grade, AkzoNobel HPMO) and demineralized water at a deposition temperature of 120 ºC. For the hybrid ALD/MLD growth of the alucone layers, ethylene glycol (EG) or 1,5 pentanediol (PD) (both from Sigma-Aldrich) were implemented as co-reactants along with TMA. The TMA and water were contained in stainless steel bubblers and vaporization was carried at 30 ºC. The diols were vaporized at 80 ºC (EG) and 120 ºC (PD) respectively. All the precursor transport lines were heat-traced at a temperature above the vaporization temperature in order to prevent precursor condensation. Dry nitrogen (HiQ 5.0, Linde Gas Benelux) was used for fluidization, purging of the reactor and transport lines and as a precursor carrier gas. The prepared catalysts were calcined in a furnace using a heating rate of 10 K/min and a final temperature of 700 ºC or 800 ºC with a hold time of 2 hours. Subsequently the catalysts were cooled down to room temperature.

The Pt and Al content of the catalysts was measured by inductively coupled plasma atomic emission spectroscopy (ICP-AES) in a PerkinElmer Optima 4300 spectrometer. Bright-field transmission electron microscopy (TEM) in a JEOL JEM 1400 microscope was used for probing the Pt cluster size and the thicknes of the Al_2O_3 and alucone overcoats. The obtained images were processed with ImageJ in order to derive particle size distributions for the metal clusters. Nitrogen adsorption and BET surface area analysis was performed in a Micromeritics TriStar II 3020. CO adsorption measurements were carried at the reduced samples (H_2, 350 ºC) in a Micromeritics ASAP 2020.

3 RESULTS AND DISCUSSION

The model supported Pt catalysts were synthesized on TiO_2 nanoparticles using a reported method [26]. The deposited Pt clusters were 1.5-2.0 nm in diameter for both loadings of 0.45 and 0.74 wt.% Pt obtained by varying the total Pt precursor exposure. The specific surface area of the support nanoparticles remained effectively unchanged (54 m^2/g) after the deposition of the active phase.

For conventional ALD overcoating schemes, variation of the number of applied cycles will result in the growth of ultrathin protective films of different thickness. The growth-per-cycle (GPC) is influenced by certain support- and process-related parameters (e.g. availability of OH active sites, reaction temperature) and in general it is accepted that a full Al_2O_3 monolayer (3.8 Å) can only be achieved after 3-4 cycles [27]. Sequential exposure of TMA and H_2O for 2 cycles is expected to result in the formation of discontinuous Al_2O_3 patches instead of a film [16]. Based on the Al content of the catalysts a GPC of 0.8 Å was estimated after 15 cycles. This is slightly lower than our previous reported value (1.4Å) for growth at ambient conditions [25]. The linear increase of the amount of material deposited, as measured by ICP, versus the number of ALD cycles (5-25) performed is shown in figure 1.

The thickness of the grown protective films was verified by TEM measurements. A thickness of ~1.9 nm was estimated (TEM) for the sample prepared after 15 ALD cycles. The discrepancy between the value estimated from ICP and TEM can be tentatively attributed to assumptions during the conversion of the Al content to film thickness. Deviations from the density value of 2.8 g/cm^3 [28] that was selected based on the growth temperature of 120 ºC and the assumption of spherical shape of the support particles can be expected. The overcoats lead to an increase of the primary particle size, as indicated by the measured value of the BET specific surface area of 41 m^2/g for the 15-cycle sample.

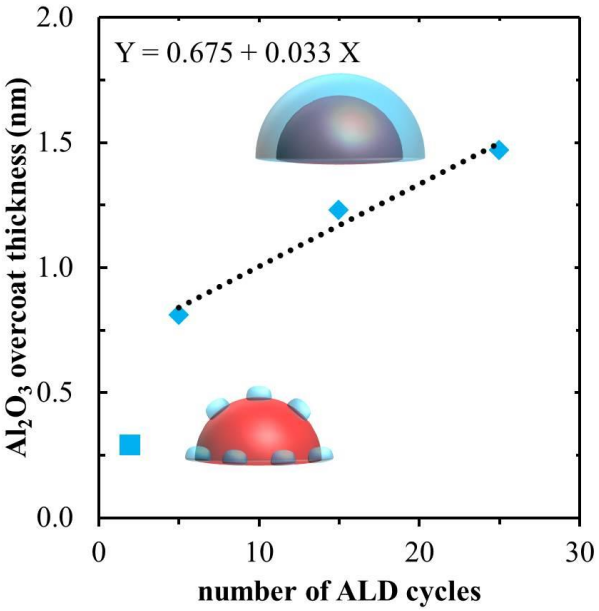

Figure 1: Thickness of Al_2O_3 overcoats versus ALD cycles (square, ■ corresponds to patches deposition; diamonds, ♦ correspond to film deposition).

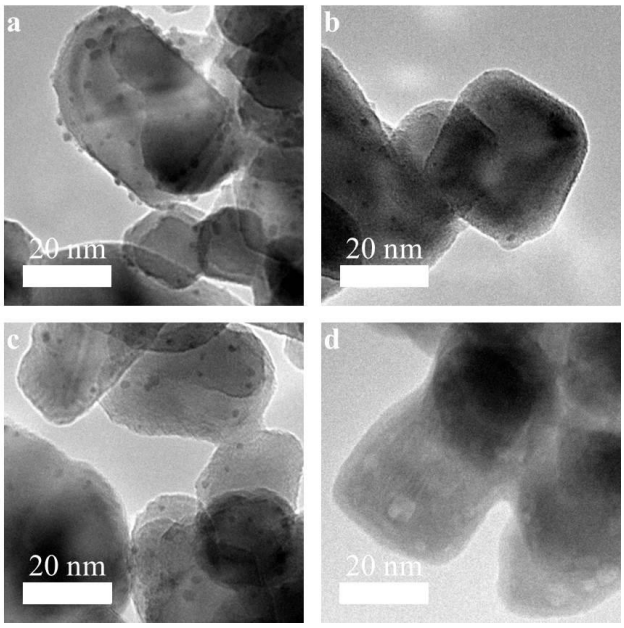

Figure 2: TEM images: (a) $2AlO_x$-Pt/TiO_2; (b) $15AlO_x$-Pt/TiO_2; (c) $15AlO_x$-Pt/TiO_2-800ºC; (d) sub-saturated (0.75min H_2O pulse) 0.75sub_$15AlO_x$-Pt/TiO_2.

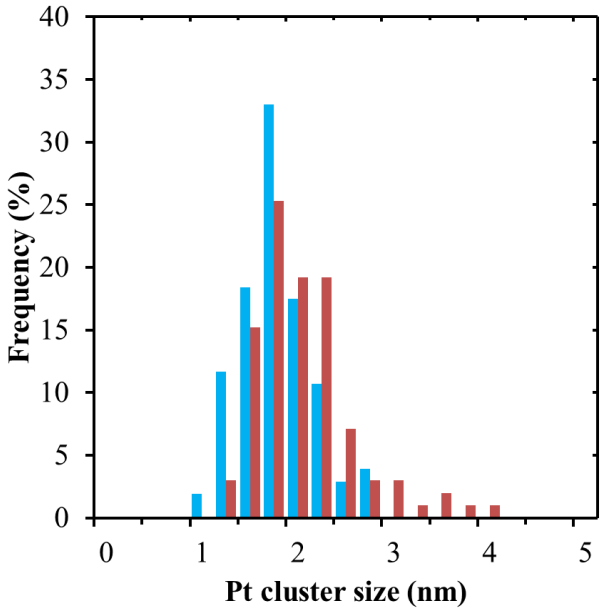

Figure 3: Size distribution histogram of Pt clusters for a sample of 2 ALD overcoat cycles (blue) and a calcined sample of 15 ALD overcoat cycles (red).

Additionally, samples with sub-saturative co-reactant (H_2O) pulses were prepared in order to study the effect of incomplete ligand removal to the subsequent porosity induction during calcination. Two overcoat experiments were performed with exposure time of ½ and ⅓ of the base case (1.5 min). In that way, films of 1.4-2.2 nm were obtained. These samples indicated some non-conformal growth features as shown in figure 2 (d). By utilizing a hybrid ALD/MLD scheme, composite films were also grown following the same pulsing sequence with the base case but for 8 cycles. The use of diols (EG and PD) as co-reactants instead of H_2O lead generally to lower growth.

In order to induce porosity to the coatings, selected samples were exposed to air in high-temperature. This is expected to crack the coatings open due to the removal of trapped H_2O and remaining organic ligands. No significant changes in the BET surface area of the samples (40 m^2/g) were observed after the calcination. The particle size distribution of the Pt species was derived from TEM images [Figure 2 (a) and (c)] before ($2AlO_x$-Pt/TiO_2) and after ($15AlO_x$-Pt/TiO_2-800ºC) the calcination process. As shown in figure 3, the average Pt cluster size slightly grew from 1.7 nm to 1.9 nm. The overcoat can thus protect to a certain extent the underlying Pt clusters. Optimizing the overcoat thickness will enhance further the thermal stability of the active metal phase.

The total adsorption of CO indicated that the 15-cycle overcoat [shown in figure 2 (b)] blocked some of the Pt clusters. Calcination of the samples induced accesibility to the clusters (metal surface area increased from 0.32 to 0.83 m^2/g catalyst). However, the results for CO chemisorption (table 2), indicated that for the overcoated sample ~25% of the Pt clusters were still accesible. That amount was decreased to 0.03 m^2/g in the calcined catalyst. A possible explanation is that calcination at the crystallization temperature (800 ºC) resulted in densification of the AlO_x phase [29]. Repetition of the measurements under different overcoat thickness values is expected to elucidate the effect of the overcoat in the stability of the metal clusters.

catalyst	Total adsorption [m^2/g catalyst	Chemisorption [m^2/g catalyst]
Pt/TiO_2	2.47	0.51
$15AlO_x$-Pt/TiO_2	0.32	0.12
$15AlO_x$-Pt/TiO_2-800ºC	0.83	0.03

Table 2: Total CO adsorption and chemisorption amounts for i) the as-deposited, ii) overcoated (15 cycles) and iii) calcined (800ºC) overcoated (15 cycles) catalysts.

4 CONCLUSIONS

We have demonstrated several nanostructuring concepts (*viz.* alteration of overcoat thickness for 2-25 cycles of conventional ALD, incomplete films by sub-saturation of the co-reactant (H_2O) pulse, hybrid MLD growth of alucone layers) coupled with porosity induction *via* heat treatment (calcination at 700 ºC and 800 ºC) can result to stabilization of the metal active phase against thermal sintering. Tuning the film characteristics can further improve the stability of the catalysts. ALD/MLD in fluidized bed or spatial ALD reactors is a promising fabrication route for preparing precisely tailored heterogeneous catalysts.

ACKNOWLEDGEMENTS

The research leading to these results has received funding from the European Research Council under the European Union's Seventh Framework Programme (FP/2007-2013)/ERC Grant, Agreement No. 279632.

REFERENCES

[1] F. Zaera, Catalysis Letters, 142, 501, 2012.
[2] M. D. Argyle, C. H. Bartholomew, Catalysts, 5, 145, 2015.
[3] J. Lu, J. W. Elam, P. C. Stair, Accounts of Chemical Research, 2013.
[4] J. Lu, K.-B. Low, Y. Lei, J. A. Libera, A. Nicholls, P. C. Stair, J. W. Elam, Nature Communications, 5, 2014.
[5] N. A. Ray, R. P. Van Duyne, P. C. Stair, The Journal of Physical Chemistry C, 116, 7748, 2012.
[6] H. Feng, J. W. Elam, J. A. Libera, W. Setthapun, P. C. Stair, Chemistry of Materials, 22, 3133, 2010.
[7] H. Feng, J. A. Libera, P. C. Stair, J. T. Miller, J. W. Elam, ACS Catalysis, 1, 665, 2011.
[8] H. Feng, J. Lu, P. C. Stair, J. W. Elam, Catalysis Letters, 141, 512, 2011.
[9] N. Cheng, M. N. Banis, J. Liu, A. Riese, X. Li, R. Li, S. Ye, S. Knights, X. Sun, Advanced Materials, 27, 277, 2015.
[10] T. D. Gould, A. Izar, A. W. Weimer, J. L. Falconer, J. W. Medlin, ACS Catalysis, 4, 2714, 2014.
[11] X. Liang, J. Li, M. Yu, C. N. McMurray, J. L. Falconer, A. W. Weimer, ACS Catalysis, 1, 1162, 2011.
[12] Z. Shang, R. L. Patel, B. W. Evanko, X. Liang, Chemical Communications, 49, 10067, 2013.
[13] H. Yi, H. Du, Y. Hu, H. Yan, H.-L. Jiang, J. Lu, ACS Catalysis, 2735, 2015.
[14] B. Fu, J. Lu, P. C. Stair, G. Xiao, M. C. Kung, H. H. Kung, Journal of Catalysis, 297, 289, 2013.
[15] J. Lu, B. Fu, M. C. Kung, G. Xiao, J. W. Elam, H. H. Kung, P. C. Stair, Science, 335, 1205, 2012.
[16] J. Lu, B. Liu, J. P. Greeley, Z. Feng, J. A. Libera, Y. Lei, M. J. Bedzyk, P. C. Stair, J. W. Elam, Chemistry of Materials, 24, 2047, 2012.
[17] H. Zhang, X.-K. Gu, C. Canlas, A. J. Kropf, P. Aich, J. P. Greeley, J. W. Elam, R. J. Meyers, J. A. Dumesic, P. C. Stair, C. L. Marshall, Angewandte Chemie International Edition, 53, 12132, 2014.
[18] A. C. Alba-Rubio, B. J. O'Neill, F. Shi, C. Akatay, C. Canlas, T. Li, R. Winans, J. W. Elam, E. A. Stach, P. M. Voyles, J. A. Dumesic, ACS Catalysis, 4, 1554, 2014.
[19] J. Lee, D. Jackson, T. Li, R. E. Winans, J. Dumesic, T. Kuech, G. Huber, Energy & Environmental Science, 2014.
[20] B. J. O'Neill, D. H. K. Jackson, A. J. Crisci, C. A. Farberow, F. Shi, A. C. Alba-Rubio, J. Lu, P. J. Dietrich, X. Gu, C. L. Marshall, P. C. Stair, J. W. Elam, J. T. Miller, F. H. Ribeiro, P. M. Voyles, J. Greeley, M. Mavrikakis, S. L. Scott, T. F. Kuech, J. A. Dumesic, Angewandte Chemie International Edition, 52, 13808, 2013.
[21] B. J. O'Neill, J. T. Miller, P. J. Dietrich, F. G. Sollberger, F. H. Ribeiro, J. A. Dumesic, ChemCatChem, 6, 2493, 2014.
[22] B. J. O'Neill, C. Sener, D. H. K. Jackson, T. F. Kuech, J. A. Dumesic, ChemSusChem, 7, 3247, 2014.
[23] H. Zhang, Y. Lei, A. J. Kropf, G. Zhang, J. W. Elam, J. T. Miller, F. Sollberger, F. Ribeiro, M. C. Akatay, E. A. Stach, J. A. Dumesic, C. L. Marshall, Journal of Catalysis, 317, 284, 2014.
[24] B. J. O'Neill, D. H. K. Jackson, J. Lee, C. Canlas, P. C. Stair, C. L. Marshall, J. W. Elam, T. F. Kuech, J. A. Dumesic, G. W. Huber, ACS Catalysis, 5, 1804, 2015.
[25] D. Valdesueiro, G. Meesters, M. Kreutzer, J. van Ommen, Materials, 8, 1249, 2015.
[26] A. Goulas, R. J. van Ommen, Journal of Materials Chemistry A, 1, 4647, 2013.
[27] S. M. George, Chemical Reviews, 110, 111, 2010.
[28] M. D. Groner, F. H. Fabreguette, J. W. Elam, S. M. George, Chemistry of Materials, 16, 639, 2004.
[29] V. Cimalla, M. Baeumler, L. Kirste, M. Prescher, B. Christian, F. Passow, F. Benkhelifa, F. Bernhardt, G. Eichapfel, M. Himmerlich, S. Krischok, J. Pezoldt, Materials Sciences and Applications, 5, 628, 2014.